AJRCMB Articles in Press. Published on 10-August-2018 as 10.1165/rcmb.2018-0123OC

# Immune Checkpoint Ligand PD-L1 Is Upregulated in Pulmonary Lymphangioleiomyomatosis (LAM)

Katharina Maisel[1#*], Mervyn J. Merrilees[2*], Elena N. Atochina-Vasserman[3*], Lurong Lian[3], Kseniya Obraztsova[3], Ryan Rue[3], Alexander N. Vasserman[3], Ning Zuo[2], Luis F. Angel[4], Andrew J. Gow[5], Inkyung Kang[6], Thomas N. Wight[6], Evgeniy Eruslanov[7], Melody A. Swartz[1], and Vera P. Krymskaya[3#]

[1]Institute for Molecular Engineering, University of Chicago, Chicago, IL; [2]Department of Anatomy and Medical Imaging, School of Medical Sciences, University of Auckland, Auckland, New Zealand; [3]Penn Center for Pulmonary Biology, Pulmonary, Allergy and Critical Care Division, University of Pennsylvania Perelman School of Medicine, Philadelphia, PA; [4]New York University Langone Medical Center, New York, NY; [5]Department of Pharmacology & Toxicology, Ernest Mario School of Pharmacy, Rutgers University, Piscataway, NJ; [6]Matrix Biology Program, Benaroya Research Institute, Seattle, WA; [7]Department of Surgery, University of Pennsylvania Perelman School of Medicine, Philadelphia, PA

* - Authors who contributed equally to the study

**# Corresponding authors:**

Katharina Maisel, PhD

Institute for Molecular Engineering
University of Chicago
Eckhardt Research Center 318
5640 S. Ellis Avenue
Chicago, IL
Phone: 773-834-0578
E-mail: maiselka@uchicago.edu

Vera P. Krymskaya, PhD, MBA, FCPP

University of Pennsylavana
219 Stemmler Hall
3450 Hamilton Walk
Philadelphia, PA 19104
Phone (office): 215-573-9861
Phone (lab): 215-746-3599
Fax: 215-746-0376
E-mail:
krymskay@pennmedicine.upenn.edu

**Running Title:** PD-L1 in LAM

**Funded by**: National Institutes of Health/National Heart, Lung and Blood Institute and National Institute for Allergy and Infectious Diseases grants: R01 HL114085 (VPK), R01 HL131626 (VPK), R21 AI130821 (MAS), T32 HL07605 (KM), F32 HL134251 (KM), and P01 HL098067 (TNW); The LAM Foundation Pilot Award LAM0121P01-17 (VPK); The New Zealand LAM Charitable Trust (MM).

Authors' contributions were as follows: conception and design, KM, MM, KO, LL, EA-V, MAS, VPK; acquisition of data, KM, LL, KO, EA-V, RR, LA, NZ, MM, IK, EE; analysis and interpretation, KM, LL, KO, EA-V, MM, IK, AG, TNW, EE, MAS, VPK; drafting the manuscript for important intellectual content, KM, MM, EE, MAS, VPK; and final approval of the manuscript, all authors.



Copyright © 2018 by the American Thoracic Society

## ABSTRACT

Pulmonary lymphangioleiomyomatosis (LAM) is a slow-progressing metastatic disease that is driven by mutations in the tumor suppressor tuberous sclerosis complex 1/2 (TSC1/2). Rapamycin inhibits LAM cell proliferation and is the only approved treatment, yet it can only stabilize the disease but not cause regression of existing lesions. However, in other cancers, immunotherapies such as checkpoint blockade against PD-1 and its ligand PD-L1 have shown promise in causing tumor regression and even curing some patients. Thus, we asked whether PD-L1 has a role in LAM progression. *In vitro*, PD-L1 expression in murine Tsc2-null cells is unaffected by mTOR inhibition with torin, but can be upregulated by IFN-γ. Using immunohistochemistry and single cell flow cytometry, we report increased PD-L1 expression in both human lung tissue from LAM patients as well as in Tsc2-null lesions in a murine model of LAM. In this model, PD-L1 is highly expressed in the lung by antigen-presenting and stromal cells, and activated T cells expressing PD-1 infiltrate the affected lung. *In vivo* treatment with anti-PD-1 antibody significantly prolongs mouse survival in the model of LAM. Together, these data demonstrate that PD-1-/PD-L1-mediated immunosuppression may occur in LAM and suggest new opportunities for therapeutic targeting that provide benefits beyond those of rapamycin.


**Keywords:** immune suppression, TSC2, mTOR, torin, PD-1, mouse, human



Copyright © 2018 by the American Thoracic Society

AJRCMB Articles in Press. Published on 10-August-2018 as 10.1165/rcmb.2018-0123OC

## INTRODUCTION

Pulmonary lymphangioleiomyomatosis (LAM), a rare genetic lung disease affecting primarily women of reproductive age, is characterized by the growth of atypical smooth muscle (SM)-like LAM cells forming microscopic lesions within lungs and axial lymphatics (1). LAM is characterized by cystic destruction of the lung interstitium, obstruction of pulmonary lymphatics, and progressive loss of lung function. Marked progress has been made in the understanding of LAM etiology by linking inactivating mutations of the tumor suppressor genes *tuberous sclerosis complex 1* (*TSC1*) and *TSC2* to the constitutive activation of the mammalian/mechanistic target of rapamycin complex 1 (mTORC1) with neoplastic LAM cell growth (2-5). Successful preclinical and clinical studies targeting mTORC1 culminated in FDA approval of the mTOR inhibitor rapamycin (sirolimus) as the first treatment for LAM in 2015 (6). Rapamycin, however, only slows disease progression, and incomplete responses are common (7, 8). Thus, there remains an urgent need to identify new targets for development of curative LAM treatment.

Recently, immunotherapies have emerged as promising treatments for various diseases including neoplastic tumors (9, 10). These treatments seek to re-activate anti-tumor immune responses that were shut off by immune evasive mechanisms induced by the tumors (9). Various mechanisms have been found in tumors to evade the immune system: 1) downregulation or loss of neo-antigens, 2) enhancement of resistance to immune cell-induced cytotoxicity via anti-apoptotic mechanisms, 3) inhibition of T cell entry, 4) suppression of cytotoxic functions of T cells through recruitment of anti-inflammatory cells like myeloid-derived suppressor cells, and 5)



Copyright © 2018 by the American Thoracic Society

induction of T cell anergy or exhaustion by activating checkpoint molecules like programmed cell death protein 1 (PD-1) and cytotoxic T lymphocyte associated antigen 4 (CTLA-4) (10-14) . While many studies have focused on understanding the tumor immune microenvironment, our knowledge and understanding of immunity in LAM is very limited (1). An important unanswered question is how LAM cells escape detection and elimination by the immune system (14). Studies have demonstrated that LAM cells express melanoma antigens like ganglioside D3 and gp100 (15, 16), suggesting that LAM cells may be susceptible to cytotoxic lymphocytes. LAM cells have also been shown to express the pro-oncogenic transcription factor STAT3, sustaining their survival (17, 18). However, it is unclear how LAM cells escape immune surveillance. Interestingly, type II interferon $\gamma$ (IFN$\gamma$), which is known to suppress cancer cell growth, had very limited inhibitory effect on uncontrolled LAM cell growth in culture (17), suggesting that LAM cells can develop a resistance to immune cytotoxicity mediated by IFN$\gamma$. LAM lesions may also change their microenvironment by recruiting tumor-associated macrophages (19) and stromal fibroblasts (20). In addition, elevated levels of natural killers (NK) cell activating receptor and their ligands in LAM tissue and serum suggest a role for the innate immune system in LAM (21). However, the potential clinical application of immunomodulatory approaches for treatment of LAM requires further investigation into the role of immunity in LAM.

In cancer, checkpoint blockade has proven to be among the most effective immunotherapeutic treatment (10-13). Among these, the most clinically validated are antibodies that block PD-1 or PD-1 ligand [PD-L1 or B7 homolog 1 (B7-H1)] axis. PD-L1 is upregulated in some tumor microenvironments – on tumor cells, stromal cells and/or



Copyright © 2018 by the American Thoracic Society

AJRCMB Articles in Press. Published on 10-August-2018 as 10.1165/rcmb.2018-0123OC

antigen-presenting cells – and the interaction of PD-L1 with PD-1 on T cells is a potent driver of T cell anergy and exhaustion (10). Thus, therapeutic blockade of these molecules (e.g., with blocking antibodies) can stimulate anti-tumor immunity (10, 12). Anti-PD-1 therapy has proven particularly effective in subsets of patients with non-small cell lung cancers, metastatic melanoma, Hodgkin's lymphoma, and bladder cancer (22). Furthermore, unlike cell-based therapies, engineered T cells or dendritic cell vaccines, checkpoint blockade is far easier to administer in non-specialized centers, and, as a result, leading to the most clinical trials of any immunotherapy (23, 24). In this study, we examined the expression patterns of PD-L1 protein in lung tissue from patients with LAM, in TSC2-null cells, and in an immunocompetent murine model of LAM. Furthermore, we assessed T cell infiltration in our murine model and investigated the potential of using immunotherapies, here anti-PD-1 treatment, as a novel therapy for treating LAM.



Copyright © 2018 by the American Thoracic Society

## MATERIALS AND METHODS

**Immunohistochemical/Immunofluorescence analysis.** Lung tissue samples from 6 patients with advanced LAM disease and 4 controls were received from the National Disease Research Interchange (NDRI) and University of Texas Health Science Center in compliance with University of Pennsylvania Review Board approved procedures. Immunohistochemistry/Immunofluorescence was performed using antibodies against human PD-L1 (E1L3N) XP (Cell Signaling Technology, Inc., Beverly, MA, USA), or murine PD-L1 (Novus Biologicals, Littleton, CO, USA), phospho-ribosomal protein S6 (pS6) (Cell Signaling Technology, Inc., Beverly, MA, USA), smooth muscle (SM) $\alpha$-actin (Sigma Chemical Co., St. Louis, MO, USA), and prospero homeobox protein 1 (Prox1) (Abcam, ab199359 clone Epr19273). Images were analyzed using Aperio ImageScope software (Leica Biosystems Imaging, Inc., Buffalo Grove, IL, USA) and quantified images using FIJI deconvolution software.

**Immunocompetent mouse model of LAM.** To study the immune involvement in LAM, we developed a metastatic model of LAM in immunocompetent C57BL/6 mice. We examined lung lesion formation induced by Tsc2-null kidney-derived epithelial tumor TTJ cells derived from *Tsc2*$^{-/+}$ C57Bl/6 mice first in immunodeficient nude BALB/c mice, and then in C57BL/6 mice. As controls, we used Tsc2-expressing mouse kidney tubular epithelial TM1 cells and Lewis lung carcinoma (LLC) cells, an established model of mouse lung cancer (25). Detailed description of generating TTJ and TM1 cells and establishing the immunocompetent mouse model of LAM is included in the Online Supplemental Materials. All animal procedures were performed according to a protocol approved by the University of Pennsylvania Animal Care and Use Committee (IACUC).



Copyright © 2018 by the American Thoracic Society

AJRCMB Articles in Press. Published on 10-August-2018 as 10.1165/rcmb.2018-0123OC

***In vivo* treatment with anti-PD-1 antibody.** Mice were treated with either with 300 μg/mouse anti-mouse PD-1 antibody (CD279) (RMP1-14) (BioXCell, West Lebanon, NH, USA) (n=20) or with 300 μg/mouse anti-mouse control IgG2a (BioXCell) (n=10) by i.p. injection twice a week. Treatment started at 10 days post tail vein injection of $10^6$ TTJ cells in C57BL/6 mice. Animals were observed by monitoring their weights, and were sacrificed at approximately 20% loss of body weight in accordance with our IACUC protocol. Lungs were inflated under 25 $cm^2$ $H_2O$ pressure and fixed for morphological and immunohistochemical analysis as described (19).

**Flow cytometry.** In human LAM lungs, the expression of PD-L1 and CD14 was analyzed by flow cytometry of single cell suspensions prepared as previously described (26, 27). Mouse lungs were digested into single cell suspensions and cells were stained with antibodies for appropriate markers to identify cell types including T cells, stromal cells, and antigen-presenting cells. Antibodies were purchased from Biolegend (San Diego, CA, USA) or eBiosciences at Thermo Fisher (Waltham, MA, USA).

**Data analysis.** Data points from individual assays represent mean $\pm$ SE. Statistically significant differences among groups were assessed with the analysis of variance (ANOVA) (with the Bonferroni-Dunn correction), Kaplan Meier (with Log-Sum Rank analysis) or student's t-test, with values of $p<0.05$ sufficient to reject the null hypothesis for all analyses.

*For further detailed methods (including cell culture, the immunocompetent mouse model of LAM, flow cytometry, western blotting, and qRT-PCR), please see the Online Data Supplement.*



Copyright © 2018 by the American Thoracic Society

## RESULTS

**PD-L1 expression and T cell infiltration in human LAM lung lesions.** We performed immunohistochemical (IHC) staining of tissue sections from distal lungs, obtained from LAM transplant patients, to determine whether LAM cells expressing smooth muscle (SM) $\alpha$-actin and phospho-ribosomal protein S6 (pS6), a biomarker of TSC2 loss and mTORC1 activation, also express PD-L1. IHC specific staining of control lung tissue (Figure 1A, upper panels) compared to LAM lung tissue (Figure 1A, lower panels) highlight typical LAM cell nodules (arrows). Marked reactivity for PD-L1 was also detected in some LAM nodules (Figure 1A, lower panel), while PD-L1 staining was significantly lower in lung sections from healthy controls (Figure 1A, upper panel, and Figure 1B). To determine specificity of PD-L1 staining to LAM disease, we performed IHC analysis of lung sections from patients with cystic fibrosis and smooth muscle cells of aorta and bronchus. PD-L1 was not detected in these samples (data not shown).

In addition to the LAM cell nodules found in LAM lungs, metastasizing LAM cell clusters have been detected in chylous pleural fluid and in the lumen of the thoracic duct of patients with LAM (28). These clusters are covered by VEGFR3-positive lymphatic endothelial cells (29) which might prevent immune detection of LAM cells, facilitating their uncontrolled growth, survival and metastasis (30, 31). In our study, we identified LAM cell nodules positive for pS6 and SM $\alpha$-actin, which showed also immunoreactivity for PD-L1 and lymphatic endothelial marker Prox-1 (Figure 1B). Quantitative analysis of IHC staining using FIJI deconvolution software demonstrated statistically significant PD-L1 upregulation in LAM nodules and LAM lung interstitium



Copyright © 2018 by the American Thoracic Society

AJRCMB Articles in Press. Published on 10-August-2018 as 10.1165/rcmb.2018-0123OC

compared to control lung interstitium (Figure 1C).

PD-L1 upregulation was further demonstrated by flow cytometry analysis of single cell suspension obtained by enzymatic digestion of LAM lungs. LAM lung cells, gated on all live cells (left column), demonstrated elevated expression of PD-L1 in both CD14-positive (CD14+) and CD14-negative (CD14-) populations compared to peripheral blood monocytic cells (PBMCs) from the same LAM patients used as controls (Figure 1D). A high level of PD-L1 was associated with CD14+ monocytes/macrophages in LAM tissue compared to peripheral blood CD14+ cells (Figure 1D, red box). Expression of PD-L1 at a lower level was also found on other CD14- cells (Figure 1D, blue box) consistent with PD-L1 expression in LAM lung.

Since PD-1-/PD-L1-based immune suppression requires direct interaction between cells expressing PD-L1 and T cells expressing PD-1, we assessed co-localization of these cells in LAM lungs. We show that CD3+ T cells infiltrate pS6 positive LAM lesions (Figure 1E, images are consecutive slices), indicating that T cell-LAM cell interactions may occur and could modulate the T cell response in LAM.

**PD-L1 upregulation in Tsc2-null TTJ lesions in the immunocompetent mouse model of LAM**. Preclinical testing of anti-PD-1/PD-L1 antibodies for potential immune targeting therapies of LAM requires availability of an immunocompetent mouse model of LAM. Since genetic deletion of either *Tsc2* or *Tsc1* is embryonically lethal and heterozygous animals do not recapitulate LAM disease (32), our efforts have focused on generating a Tsc2-null lung tumor model similar to LAM. A mouse model of experimental metastasis of Tsc2-null cells to the lung could recapitulate the proposed metastatic model of LAM, which postulates that, in some patients, cells with TSC2



Copyright © 2018 by the American Thoracic Society

mutations from kidney metastasize to the lung (25). Our initial efforts to generate a xenograft model in severe combined immunodeficiency (SCID) mice using primary human LAM cells showed that, when cells were injected into the tail vein, only a few LAM cells were detected in the lung after months of observations with no evidence of progressive growth (unpublished data). These observations suggest that primary human LAM cells do not grow in the lung even of immunocompromised mice. The possibility is that LAM cells can trigger innate immune tumor suppression even in an adaptive immune compromised environment.

To develop an experimental metastatic model of LAM with Tsc2-null lung lesions in immunocompetent C57BL/6 mice, we used Tsc2-null TTJ cells, which show mTORC1 activation (Figure 2A). TTJ cells were generated by successive propagation of the original Tsc2-null MKOC cells derived from mouse kidney lesions that spontaneously develop in heterozygous *Tsc2*$^{+/-}$ C57BL/6 mice (32, 33) schematically represented in Figure 2B and described in the Online Data Supplement. The original Tsc2-null MKOC cells underwent *in vivo* immune-editing producing TTJ cells by sequential propagation in immunodeficient nude BALB/c background and immunocompetent C57BL/6 mice. This approach allows selection for growth of tumor variants that escape from immune suppression (14).

We first sought to test if, when cultured *in vitro*, mouse MKOC and TTJ cells [compared to Tsc2-expressing M1 cells and *Tsc2*$^{-/-}$ and *Tsc2*$^{+/+}$ mouse embryonic fibroblasts (MEFs)] express PD-L1 and MHCI molecules, which would allow for direct interaction with the T cell receptor and subsequent suppression of T cells along the PD-1/PD-L1 axis. In addition, since it is well established that IFN$\gamma$ produced by cytotoxic T



Copyright © 2018 by the American Thoracic Society

AJRCMB Articles in Press. Published on 10-August-2018 as 10.1165/rcmb.2018-0123OC

cells prevents tumor development by immune evasion, we also determined if IFNγ stimulation would enhance PD-L1 and MHCI expression similar to what is seen in stromal cells (34). Our analysis demonstrates that both Tsc2-expressing (M1 and *Tsc2*$^{+/+}$ MEFs) and Tsc2-deficient cells (MKOC, TTJ, and *Tsc2*$^{-/-}$ MEFs) express low levels of PD-L1 and MHCI at baseline, and that this expression is significantly potentiated by stimulation with IFNγ (Figure E2). Interestingly, the Tsc2-null cells derived from mouse kidney lesions (MKOC and TTJ) had ~4-5-fold higher PD-L1 expression upon IFNγ stimulation compared to Tsc2-expressing M1 cells (Figure E2A). Expression patterns were minimally affected or increased by mTORC1 inhibition with torin in mouse cells, both at baseline and after IFNγ stimulation (Figures E2B, E2D, and E2F). Interestingly, in MEFs, mTORC1 inhibition with torin significantly increased MHCI expression upon IFNγ stimulation (Figure E2H), a phenomenon we are now investigating. PD-L1 expression was confirmed by qRT-PCR (Figure E3).

When we tail vein-injected Tsc2-null TTJ cells to form a mouse model of metastatic LAM, we saw multiple lesions covering 50.7±6.6% of total lung in nude mice (Figures 2C and 2D). In contrast, the same number of TTJ cells injected in C57BL/6 mice formed significantly fewer lesions (21.5±4.6%) (Figures 2C, 2D and Figure E4) likely due to both the very different phenotype of BALB/c-derived nude mice and C57BL/6 mice and increased immune suppression of Tsc2-null lung tumors in immunocompetent C57BL/6 mice. Immunohistochemical staining showed mTORC1 activation detected by pS6 immunoreactivity, SM α-actin and PD-L1 expression in Tsc2-null TTJ lesions in lungs from C57BL/6 mice (Figures 2E and E5). CD3-positive T cell infiltrates were also



Copyright © 2018 by the American Thoracic Society

detected near Tsc2-null TTJ lesions (Figure 2E), suggesting that interaction between T cells and Tsc2-null may modulate T cell activation and tumor growth.

**Antigen-presenting cells infiltrate mouse lungs with Tsc2-null lesions and express high levels of PD-L1 in a murine model of LAM**. We investigated lung infiltration of antigen-presenting cells (APCs), the cell types known for their interactions with lymphocytes, and their PD-L1 expression in the metastatic mouse model of LAM with Tsc2-null lung lesions. We found marked increases in dendritic cells, both CD11b-positive (CD11b+) and CD11b-negative (CD11b-) subtypes, monocytes, and macrophages in mouse lungs with Tsc2-null lesions compared to controls (Figure 3A). PD-L1 expression is increased in the various APC populations in the lungs from the mouse model of LAM (Figure 3B, upper panels), as evident in the shift of fluorescence intensity (representative histograms are shown in Figure 3B, upper panels, red = LAM model with Tsc2-null lesions, blue = control lung), and this difference was statistically significant when quantified via flow cytometry (Figure 3B, lower panels). Interestingly, PD-L1 expression was also significantly increased in CD45-negative (CD45-) stromal cell populations including CD140a-positive (CD140a+) fibroblasts, epithelial cells, and CD31-negative (CD31-) cells (that include Tsc2-null TTJ cells in the mouse model of LAM) (Figure 3C). Overall, our data indicate that high levels of PD-L1 expression occur in stromal cells (that include Tsc2-null TTJ cells) as well as immune cells – particularly antigen-presenting cells – that can modulate T cell activation and respond to Tsc2-null TTJ cells.

**T cells expressing high levels of PD-1 infiltrate the lungs with Tsc2-null lesions.** In our previous study, we identified infiltration of innate immune cells such as



Copyright © 2018 by the American Thoracic Society

AJRCMB Articles in Press. Published on 10-August-2018 as 10.1165/rcmb.2018-0123OC

macrophages, eosinophils and neutrophils in lungs from the mouse model of LAM on BALB/c-derived nude background (19). However, little is known about the T cell response in LAM lung. We used our mouse model of LAM in immunocompetent mice to explore the adaptive immune response to LAM. Here, we found that in addition to innate cell infiltration, total T cell numbers were increased, including both CD4+ and CD8+ T cells (Figure 4A). Interestingly, we found that the distribution of T cell subsets was different in mice with Tsc2-null lesions compared to control mice. Thus, Tsc2-null lung lesions had significantly higher numbers of effector memory T cells ($T_{EM}$, both CD8+ and CD4+) compared to controls, and also show increased numbers of regulatory T cells ($T_{REGS}$, Figures 4A,B). Furthermore, CD4+ and CD8+ $T_{EM}$ in Tsc2-null lungs had significantly higher expression of PD-1, the binding partner to PD-L1, compared to control lungs (Figure 4C).

**Treatment with anti-PD-1 antibody improves survival in the mouse model of LAM.** To assess whether immunotherapeutic targeting of PD-L1 in mice with Tsc2-null lung lesions suppressed the disease, we performed a survival study comparing the effect of anti-PD-1 antibody treatment with control isotype antibody. As shown in Figure 5A, survival was significantly increased by anti-PD-1 treatment. At day 55, ~70% anti-PD-1-treated mice survived compared to only ~30% in isotype-treated mice. Further, at day 75, more than 45% of anti-PD-1-treated mice still survived, while none of the isotype-treated mice did. Morphometric analysis of lungs, taken at the time of sacrifice when animals had lost approximately 20% of weight surprisingly demonstrated that percentage of lesions per total lung was not significantly different between groups (Figure 5B). However, there was great heterogeneity of sizes and morphology of lesions



Copyright © 2018 by the American Thoracic Society

in both anti-PD-1-treated and IgG-treated lungs (Figure 5C). Collectively, our data demonstrate a significant increase of survival in mice with Tsc2-null lesions by treatment with anti-PD-1 antibody.

## DISCUSSION

Cancer immunotherapies require an existing pool of T cells that can respond to antigens specific to these cancers. These cancer antigen-specific T cells are suppressed by the immune microenvironment, but can be subsequently activated by immunotherapy (35-37). In LAM, several antigens have been identified that are also found in melanoma and neuroendocrine tumors. These include ganglioside D3 and gp100, both potential targets for natural killer T (NKT) and cytotoxic T cells (15, 38). Indeed, studies by Klarquist et al. and Gilbert et al. demonstrate that LAM cells are susceptible to NKT cell and cytotoxic lymphocyte-mediating immune targeting (15, 38). These studies also identified that despite expression of GD3, there was no NKT cell recruitment to LAM lungs. This suggests that enhancing NKT cell responses through immunization targeting GD3 may provide new therapeutic LAM treatments. However, clinical application of this approach for treatment of LAM has not been investigated (39).

Our studies have focused on classic CD8+/CD4+ T cell responses in LAM, and we have found that in our mouse model, significantly more T cells infiltrate lung with Tsc2-null lesions compared to lung of controls. In addition, we have found that these infiltrating T cells highly express PD-1, suggesting that T cells may have been shifted toward tolerance or anergy by PD-1/PD-L1 interactions (40).



Copyright © 2018 by the American Thoracic Society

AJRCMB Articles in Press. Published on 10-August-2018 as 10.1165/rcmb.2018-0123OC

Recent evidence in cancer has demonstrated that therapeutic efficacy of treatments like the anti-PD-1 therapy we have used in the present studies is highly dependent on T cell infiltration into tumors (10, 41, 42). Indeed, patients with 'hot tumors', or tumors with significant immune cell infiltrates, respond better to immune checkpoint blockade, while patients with 'cold tumors' often fall in the non-responder group. Further advances have demonstrated that the immune infiltrates are likely due to increased chemokine production in some tumors that attract immune cells (41, 43). For this reason, efforts to enhance chemokine production in tumors to transform previously 'cold' tumors into 'hot' tumors have shown significant promise. Chemokines like CCL21, which attracts CCR7+ naïve and central memory T cells along with other immune cells, have been combined with other immunotherapies as effective treatments for tumors lacking immune infiltration (44-47). Strategies such as these could potentially be applied in LAM to enhance immune infiltration into the lungs. When combined with checkpoint inhibition or other immunotherapeutic strategies, this may further enhance treatment efficacy.

The present study identifies PD-L1 as a potential novel therapeutic target in LAM. Identification of PD-L1 upregulation in LAM cell nodules demonstrates one potential mechanism of immunomodulation that may facilitate LAM cell escape from immune detection and destruction. Activation of Akt and mTOR has been linked to PD-L1 upregulation in experimental animal models and in glioma (48, 49). In LAM, mutational inactivation of TSC1/2 uncouples mTORC1 from upstream control by growth factors and nutrients leading to uncontrolled growth (1, 3, 30, 31). Our study adds to LAM pathobiology by demonstrating PD-L1 upregulation in LAM lung. In addition, we show in



Copyright © 2018 by the American Thoracic Society

Tsc2-null lesions in immunocompetent mice that there are increased levels of both innate adaptive immune cells. Further, stromal, epithelial, fibroblasts and T cells have upregulated expression of PD-L1.In this immunocompetent mouse model of metastatic LAM, treatment with anti-PD-1 antibody significantly extends mouse survival. Several important caveats of this model should be noted. Firstly, the cell of origin for the TTJ lung lesions in our model is a kidney-derived tumor. In human LAM, it is still unclear what is the source of origin of the LAM lung cells although kidney angiomyolipomas are common in this patient population. Secondly, the subcutaneous injection of Tsc2-null TTJ cells and their passaging through BALB/c-derived nude and C57BL/6 mice may have selected for particularly immune evasive cells that may respond well to immunotherapy such as anti-PD-1. Thirdly, the mouse Tsc2-null lung tumor growth is much more aggressive than lung lesion growth in LAM patients so immunotherapy may have different effects in human LAM cells with slower proliferation kinetics. Further studies are needed to identify specific molecular and cellular mechanisms of PD-L1 upregulation and its role in immunomodulation in LAM. Because blockage of the immune checkpoint axis PD-1/PD-L1 is among the most promising approaches in cancer immunotherapy, our findings also provide a new opportunity for therapeutic targeting that extends beyond the stabilization benefits of rapamycin. Such targeting may also provide an approach for those patients unresponsive to rapamycin treatment and for those with advanced LAM disease.

**Acknowledgments:** We thank Dr. Jilly Evans for critical reading of the manuscript; Mrs. Li-Ping Wang at the Pathology Clinical Service Center at the University of Pennsylvania for expert technical assistance with immunohistochemical staining of human tissue; Ms.



Copyright © 2018 by the American Thoracic Society

AJRCMB Articles in Press. Published on 10-August-2018 as 10.1165/rcmb.2018-0123OC

Jackie Yun Ying and Minmin Lu at the Histology Core at the Penn Center for Pulmonary Biology and the Cardiovascular Institute for expert assistance with immunohistochemical staining of mouse tissue.



Copyright © 2018 by the American Thoracic Society

## References

1. Krymskaya VP, McCormack FX. Lymphangioleiomyomatosis: A monogenic model of malignancy. *Annu Rev Med* 2017;68(1):69-83.
2. Carsillo T, Astrinidis A, Henske EP. Mutations in the tuberous sclerosis complex gene *tsc2* are a cause of sporadic pulmonary lymphangioleiomyomatosis. *Proc Natl Acad Sci U S A* 2000;97:6085-6090.
3. Goncharova EA, Goncharov DA, Eszterhas A, Hunter DS, Glassberg MK, Yeung RS, Walker CL, Noonan D, Kwiatkowski DJ, Chou MM, Panettieri RA, Krymskaya VP. Tuberin regulates p70 s6 kinase activation and ribosomal protein s6 phosphorylation: A role for the tsc2 tumor suppressor gene in pulmonary lymphangioleiomyomatosis. *J Biol Chem* 2002;277:30958-30967.
4. Goncharova EA, Goncharov DA, Lim PN, Noonan D, Krymskaya VP. Modulation of cell migration and invasiveness by tumor suppressor tsc2 in lymphangioleiomyomatosis. *Am J Respir Cell Mol Biol* 2006;34:473-480.
5. Crooks DM, Pacheco-Rodriguez G, DeCastro RM, McCoy JP, Jr., Wang J-a, Kumaki F, Darling T, Moss J. Molecular and genetic analysis of disseminated neoplastic cells in lymphangioleiomyomatosis. *Proc Natl Acad Sci U S A* 2004;101(50):17462-17467.
6. McCormack FX, Inoue Y, Moss J, Singer LG, Strange C, Nakata K, Barker AF, Chapman JT, Brantly ML, Stocks JM, Brown KK, Lynch JP, Goldberg HJ, Young LR, Kinder BW, Downey GP, Sullivan EJ, Colby TV, McKay RT, Cohen MM, Korbee L, Taveira-DaSilva AM, Lee H-S, Krischer JP, Trapnell BC. Efficacy and



Copyright © 2018 by the American Thoracic Society

AJRCMB Articles in Press. Published on 10-August-2018 as 10.1165/rcmb.2018-0123OC

safety of sirolimus in lymphangioleiomyomatosis. *N Engl J Med* 2011;364:1595-1606.

7. McCormack F, Gupta N, Finlay G, Young LR, Taveira-DaSilva A, Glasgow CG, Steagall WK, Johnson SR, Sahn SA, Ryu JH, Strange C, Seyama K, Sullivan EJ, Kotloff RM, Downey GP, Chapman JT, Han MK, D'Armiento J, Inoue Y, Henske EP, Bissler JJ, Colby TV, Kinder BW, Wikenheiser-Brokamp KA, Brown KK, Cordier JF, Meyer C, Cottin V, Brozek JL, Smith K, Wilson KC, Moss J. Official american thoracic society and japanise respiratory society clinical practice ghidlines: Lymphangioleiomyomatosis diagnosis and management. *Am J Respir Cell Mol Biol* 2016;194(6):748-761.
8. Krymskaya VP. Therapeutic strategies for treatment of pulmonary lymphangioleiomyomatosis. *Expert Opin Orphan Drugs* 2014;2(10):1063-1074.
9. Hanahan D, Weinberg Robert A. Hallmarks of cancer: The next generation. *Cell* 2011;144(5):646-674.
10. Pardoll DM. The blockade of immune checkpoints in cancer immunotherapy. *Nat Rev Cancer* 2012;12(4):252-264.
11. Duraiswamy J, Freeman GJ, Coukos G. Therapeutic pd-1 pathway blockade augments with other modalities of immunotherapy t-cell function to prevent immune decline in ovarian cancer. *Cancer Res* 2013;73(23):6900-6912.
12. Page DB, Postow MA, Callahan MK, Allison JP, Wolchok JD. Immune modulation in cancer with antibodies. *Annu Rev Med* 2014;65:185-202.
13. Roh W, Chen PL, Reuben A, Spencer CN, Prieto PA, Miller JP, Gopalakrishnan V, Wang F, Cooper ZA, Reddy SM, Gumbs C, Little L, Chang Q, Chen WS, Wani



Copyright © 2018 by the American Thoracic Society

K, De Macedo MP, Chen E, Austin-Breneman JL, Jiang H, Roszik J, Tetzlaff MT, Davies MA, Gershenwald JE, Tawbi H, Lazar AJ, Hwu P, Hwu WJ, Diab A, Glitza IC, Patel SP, Woodman SE, Amaria RN, Prieto VG, Hu J, Sharma P, Allison JP, Chin L, Zhang J, Wargo JA, Futreal PA. Integrated molecular analysis of tumor biopsies on sequential ctla-4 and pd-1 blockade reveals markers of response and resistance. *Sci Transl Med* 2017;9(379).

14. Schreiber RD, Old LJ, Smyth MJ. Cancer immunoediting: Integrating immunity's roles in cancer suppression and promotion. *Science* 2011;331(6024):1565-1570.

15. Klarquist J, Barfuss A, Kandala S, Reust MJ, Braun RK, Hu J, Dilling DF, McKee MD, Boissy RE, Love RB, Nishimura MI, Le Poole IC. Melanoma-associated antigen expression in lymphangioleiomyomatosis renders tumor cells susceptible to cytotoxic t cells. *Am J Pathol* 2009;175:2463-2472.

16. Gilbert ER, Eby JM, Hammer AM, Klarquist J, Christensen DG, Barfuss AJ, Boissy RE, Picken MM, Love RB, Dilling DF, Le Poole IC. Positioning ganglioside d3 as an immunotherapeutic target in lymphangioleiomyomatosis. *Am J Pathol* 2013;183(1):226-234.

17. Goncharova EA, Goncharov DA, Damera G, Tliba O, Amrani Y, Panettieri RA, Jr., Krymskaya VP. Signal transducer and activator of transcription 3 is required for abnormal proliferation and survival of tsc2-deficient cells: Relevance to pulmonary lymphangioleiomyomatosis. *Mol Pharmacol* 2009;76(4):766-777.

18. El-Hashemite N, Kwiatkowski DJ. Interferon-gamma-jak-stat signaling in pulmonary lymphangioleiomyomatosis and renal angiomyolipoma: A potential therapeutic target. *Am J Respir Cell Mol Biol* 2005;33(3):227-230.



Copyright © 2018 by the American Thoracic Society

AJRCMB Articles in Press. Published on 10-August-2018 as 10.1165/rcmb.2018-0123OC

19. Goncharova EA, Goncharov DA, Fehrenbach M, Khavin I, Ducka B, Hino O, Colby TV, Merrilees MJ, Haczku A, Albelda SM, Krymskaya VP. Prevention of alveolar destruction and airspace enlargement in a mouse model of pulmonary lymphangioleiomyomatosis (lam). *Sci Transl Med* 2012;4(154):154ra134.

20. Clements D, Dongre A, Krymskaya VP, Johnson SR. Wild type mesenchymal cells contribute to the lung pathology of lymphangioleiomyomatosis. *PLoS One* 2015;10(5):e0126025.

21. Osterburg AR, Nelson RL, Yaniv BZ, Foot R, Donica WR, Nashu MA, Liu H, Wikenheiser-Brokamp KA, Moss J, Gupta N, McCormack FX, Borchers MT. Nk cell activating receptor ligand expression in lymphangioleiomyomatosis is associated with lung function decline. *JCI Insight* 2016;1(16):e87270.

22. Page DB, Postow MA, Callahan MK, Allison JP, Wolchok JD. Immune modulation in cancer with antibodies. *Annu Rev Med* 2014;65(1):185-202.

23. Sharma P, Allison James P. Immune checkpoint targeting in cancer therapy: Toward combination strategies with curative potential. *Cell* 2015;161(2):205-214.

24. Sharma P, Allison JP. The future of immune checkpoint therapy. *Science* 2015;348(6230):56-61.

25. Hiratsuka S, Nakamura K, Iwai S, Murakami M, Itoh T, Kijima H, Shipley JM, Senior RM, Shibuya M. Mmp9 induction by vascular endothelial growth factor receptor-1 is involved in lung-specific metastasis. *Cancer Cell* 2002;2(4):289-300.

26. Quatromoni JG, Singhal S, Bhojnagarwala P, Hancock WW, Albelda SM, Eruslanov E. An optimized disaggregation method for human lung tumors that



Copyright © 2018 by the American Thoracic Society

preserves the phenotype and function of the immune cells. *Journal of Leukocyte Biology* 2014;97.

27. Eruslanov EB, Bhojnagarwala PS, Quatromoni JG, Stephen TL, Ranganathan A, Deshpande C, Akimova T, Vachani A, Litzky L, Hancock WW, Conejo-Garcia JR, Feldman M, Albelda SM, Singhal S. Tumor-associated neutrophils stimulate t cell responses in early-stage human lung cancer. *The Journal of Clinical Investigation* 2014;124(12):0-0.

28. Seyama K, Kumasaka T, Kurihara M, Mitani K, Sato T. Lymphangioleiomyomatosis: A disease involving the lymphatic system. *Lymphat Res Biol* 2010;8(1):21-31.

29. Kumasaka T, Seyama K, Mitani K, Sato T, Souma S, Kondo T, Hayashi S, Minami M, Uekusa T, Fukuchi Y, Suda K. Lymphangiogenesis in lymphangioleiomyomatosis: Its implication in the progression of lymphangioleiomyomatosis. *Am J Surg Pathol* 2004;28(8):1007-1016.

30. Henske EP, McCormack FX. Lymphangioleiomyomatosis — a wolf in sheep's clothing. *J Clin Invest* 2012;122(11):3807-3816.

31. Itkin M, McCormack FX. Nonmalignant adult thoracic lymphatic disorders. *Clin Chest Med* 2016;37(3):409-420.

32. Kwiatkowski DJ. Animal models of lam and tsc. *Lymph Res Biol* 2010;8:51-57.

33. Kobayashi T, Minowa O, Kuno J, Mitani H, Hino O, Noda T. Renal carcinogenesis, hepatic hemangiomatosis, and embryonic lethality caused by a germ-line tsc2 mutation in mice. *Cancer Res* 1999;59:1206-1211.



Copyright © 2018 by the American Thoracic Society

AJRCMB Articles in Press. Published on 10-August-2018 as 10.1165/rcmb.2018-0123OC

34. Woo SR, Corrales L, Gajewski TF. Innate immune recognition of cancer. *Annu Rev Immunol* 2015;33:445-474.

35. Peggs KS, Quezada SA, Korman AJ, Allison JP. Principles and use of anti-ctla4 antibody in human cancer immunotherapy. *Curr Opin Immunol* 2006;18(2):206-213.

36. Topalian SL, Drake CG, Pardoll DM. Targeting the pd-1/b7-h1(pd-l1) pathway to activate anti-tumor immunity. *Curr Opin Immunol* 2012;24(2):207-212.

37. Fankhauser M, Broggi MAS, Potin L, Bordry N, Jeanbart L, Lund AW, Da Costa E, Hauert S, Rincon-Restrepo M, Tremblay C, Cabello E, Homicsko K, Michielin O, Hanahan D, Speiser DE, Swartz MA. Tumor lymphangiogenesis promotes t cell infiltration and potentiates immunotherapy in melanoma. *Sci Transl Med* 2017;9(407).

38. Gilbert ER, Eby JM, Hammer AM, Klarquist J, Christensen DG, Barfuss AJ, Boissy RE, Picken MM, Love RB, Dilling DF, Le Poole IC. Positioning ganglioside d3 as an immunotherapeutic target in lymphangioleiomyomatosis. *Am J Pathol* 2013;183(1):226-234.

39. Dilling DF, Gilbert ER, Picken MM, Eby J, Love RB, Le Poole IC. A current viewpoint of lymphangioleimyomatosis supporting immunotherapeutic treatment options. *Am J Respir Cell Mol Biol* 2012;46:1-5.

40. Dong H, Strome SE, Salomao DR, Tamura H, Hirano F, Flies DB, Roche PC, Lu J, Zhu G, Tamada K, Lennon VA, Celis E, Chen L. Tumor-associated b7-h1 promotes t-cell apoptosis: A potential mechanism of immune evasion. *Nat Med* 2002;8(8):793-800.



Copyright © 2018 by the American Thoracic Society

41. Ji RR, Chasalow SD, Wang L, Hamid O, Schmidt H, Cogswell J, Alaparthy S, Berman D, Jure-Kunkel M, Siemers NO, Jackson JR, Shahabi V. An immune-active tumor microenvironment favors clinical response to ipilimumab. *Cancer Immunol Immunother* 2012;61(7):1019-1031.

42. Tumeh PC, Harview CL, Yearley JH, Shintaku IP, Taylor EJ, Robert L, Chmielowski B, Spasic M, Henry G, Ciobanu V, West AN, Carmona M, Kivork C, Seja E, Cherry G, Gutierrez AJ, Grogan TR, Mateus C, Tomasic G, Glaspy JA, Emerson RO, Robins H, Pierce RH, Elashoff DA, Robert C, Ribas A. Pd-1 blockade induces responses by inhibiting adaptive immune resistance. *Nature* 2014;515(7528):568-571.

43. Harlin H, Meng Y, Peterson AC, Zha Y, Tretiakova M, Slingluff C, McKee M, Gajewski TF. Chemokine expression in melanoma metastases associated with cd8+ t-cell recruitment. *Cancer Res* 2009;69(7):3077-3085.

44. Lin Y, Sharma S, John MS. Ccl21 cancer immunotherapy. *Cancers (Basel)* 2014;6(2):1098-1110.

45. Yang SC, Hillinger S, Riedl K, Zhang L, Zhu L, Huang M, Atianzar K, Kuo BY, Gardner B, Batra RK, Strieter RM, Dubinett SM, Sharma S. Intratumoral administration of dendritic cells overexpressing ccl21 generates systemic antitumor responses and confers tumor immunity. *Clin Cancer Res* 2004;10(8):2891-2901.

46. Kirk CJ, Hartigan-O'Connor D, Mule JJ. The dynamics of the t-cell antitumor response: Chemokine-secreting dendritic cells can prime tumor-reactive t cells extranodally. *Cancer Res* 2001;61(24):8794-8802.



Copyright © 2018 by the American Thoracic Society

AJRCMB Articles in Press. Published on 10-August-2018 as 10.1165/rcmb.2018-0123OC

47. Salehi-Rad R, Walser T, Ong S, Park S, Sharma S, Jay L, Dubinett S. Ccl21 combined with pd-1 blockade cooperatively inhibits tumor growth in kras murine model of nsclc. *Journal of Thoracic Oncology* 2017;12(8):S1537-S1537.

48. Parsa AT, Waldron JS, Panner A, Crane CA, Parney IF, Barry JJ, Cachola KE, Murray JC, Tihan T, Jensen MC, Mischel PS, Stokoe D, Pieper RO. Loss of tumor suppressor pten function increases b7-h1 expression and immunoresistance in glioma. *Nat Med* 2007;13(1):84-88.

49. Chen J, Zhang XD, Proud C. Dissecting the signaling pathways that mediate cancer in pten and lkb1 double-knockout mice. *Sci Signal* 2015;8(392):pe1-pe1.



Copyright © 2018 by the American Thoracic Society

## FIGURE LEGENDS

**Figure 1. Upregulation of PD-L1 in human LAM lung. A-B:** Representative images of IHC analysis of PD-L1 in human LAM lungs. LAM cells were detected with SM $\alpha$-actin and pS6; lymphatic endothelial cells were detected with Prox-1. Control (**A**, upper panels) – lung specimens from healthy human subjects (n=4). LAM lungs (**A**, lower panels) and (**B**) – tissue samples from human LAM lungs (n=6). Arrows indicate LAM nodules; B-bronchus, V-Vessel. **C:** Images were quantified for PD-L1 expression normalized to number of nuclei using FIJI ImageJ deconvolution software, and statistical analysis of PD-L1 IHC analysis of LAM lung (n=6) and control lung (n=4) was performed by student's *t*-test; * $p<0.05$. **D:** Flow cytometric analysis of PD-L1 expression in CD14-positive (CD14+) vs CD14-negative (CD14-) cells from single cell lung suspensions obtained from enzymatically digested LAM lung tissue (right column) (n=2), and peripheral blood monocytic cells (PBMC) served as a control (n=2). Red box - a high level of PD-L1 was associated with CD14+ monocytes/macrophages in LAM tissue compared to peripheral blood CD14+ cells. Blue box - expression of PD-L1 at a lower level was found on other CD14- cells consistent with PD-L1 expression in LAM lung nodules. FSC – forward scatter. **E:** Representative images of CD3+ cell infiltration of pS6-positive human LAM lesions (n=4).

**Figure 2. PD-L1 expression in Tsc2-null lung lesions in a metastatic immunocompetent mouse model of LAM. A:** Immunoblot analysis of Tsc2-expressing (TM1, LLC and *Tsc2*$^{+/+}$ MEFs) and Tsc2-deficient cells (TMKOC, TTJ, and *Tsc2*$^{-/-}$ MEFs with antibody against TSC2, pS6, S6, and tubulin. **B:** Schematic representation of experimental procedures establishing Tsc2-null immunocompetent



Copyright © 2018 by the American Thoracic Society

AJRCMB Articles in Press. Published on 10-August-2018 as 10.1165/rcmb.2018-0123OC

mouse LAM model. See text and Online Supplemental Materials for details. **C:** Representative H&E staining of lungs from nude mice injected with Tsc2-null TTJ cells, or C57BL/6 mice injected with either Tsc2-null TTJ or LLC cells. Animals were sacrificed at 18-21 days post-injection, lung were inflated and stained with H&E. **D:** H&E images of lung were analyzed for percentage of lesions per lung using student's t-test comparison (n=5 per each group, mean value $\pm$ SE) with p=0.04 for TTJ nude vs. TTJ C57BL/6, p=0.03 for TTJ nude vs. LLC C57BL/6. **E:** IHC analysis of pS6, SM $\alpha$-actin, PD-L1 expression and CD3-positive T cells in C57BL/6 mouse lungs with Tsc2-null lung lesions (n=5).

**Figure 3. Antigen-presenting cells infiltrate lungs with Tsc2-null lesions and highly express PD-L1. A: :** Lungs with Tsc2-null lesions taken from C57BL/6 mice sacrificed approximately 3 weeks post-injection had increased numbers of macrophage, dendritic cells (CD11b+ and CD11b-), and monocytes (activated Ly6C+ and non-activated Ly6C-). **B**: Representative histograms showing a shift in PD-L1 expression in lungs with Tsc2-null lesions (blue) compared to control lungs (red) in antigen-presenting cells, and quantification of PD-L1 expression via median fluorescence intensity (MFI) in these cell populations. **C:** PD-L1 expression in CD45-negative (CD45-) stromal cell populations including CD140a-positive (CD140a+) fibroblasts, epithelial cells, and CD31-negative (CD31-) cells that include Tsc2-null TTJ cells in the mouse model of LAM. Statistical analysis was performed using student's t-test with significance at $p<0.05$ (** $p<0.01$, *** $p<0.001$, $n\geq5$ mice, n=2 experiments).

**Figure 4. T cells infiltrate lungs with Tsc2-null lesions and highly express PD-1. A:** Lungs with Tsc2-null lesions taken from C57BL/6 mice sacrificed approximately 3



Copyright © 2018 by the American Thoracic Society

weeks post-injection have increased CD4+ and CD8+ T cells, increased CD4+ and CD8+ effector/effector memory T cells ($T_{EM}$), and regulatory T cells ($T_{REGS}$) presented as percentage of total CD4+ and CD8+ T cells. **B:** Representative flow cytometry diagrams illustrating the increase in CD4+ and CD8+ $T_{EM}$ in lungs with Tsc2-null lesions compared to controls. **C:** Quantification of overall PD-1+ CD4+ and CD8+ T cells and representative plots showing PD-1 expression on $T_{EM}$ in control lungs (red) compared to lungs with Tsc2-null lesions (blue). Statistical analysis was performed using student's t-test with significance at $p< 0.05$ (** $p<0.01$, *** $p<0.001$, $n\geq5$ mice, n=2 experiment).

**Figure 5. Anti-PD-1 antibody treatment enhances survival in a mouse model of LAM. A:** Kaplan-Meier analysis of mouse survival with Tsc2-null lung lesions. Mice were treated with either anti-PD-1 antibody (green) (n=20) or isotype control IgG2a antibody (red) (n=10). Animal survival was assessed as 20% loss of body weight. Statistical significance was determined for mice treated with anti-PD-1 antibody vs. IgG2a antibody by Log-sum rank test $p<0.0001$. **B:** Percentage of lung lesions per lung in isotype control IgG2a- and anti-PD-1-treated mice at the time of sacrifice. Statistical analysis was performed using student's t-test with $p=0.24$. **C:** Representative H&E images of lungs with Tsc2-null lesions from mice treated with either anti-PD-1 antibody or IgG2a at the time of sacrifice.



Copyright © 2018 by the American Thoracic Society

AJRCMB Articles in Press. Published on 10-August-2018 as 10.1165/rcmb.2018-0123OC

Figure 1

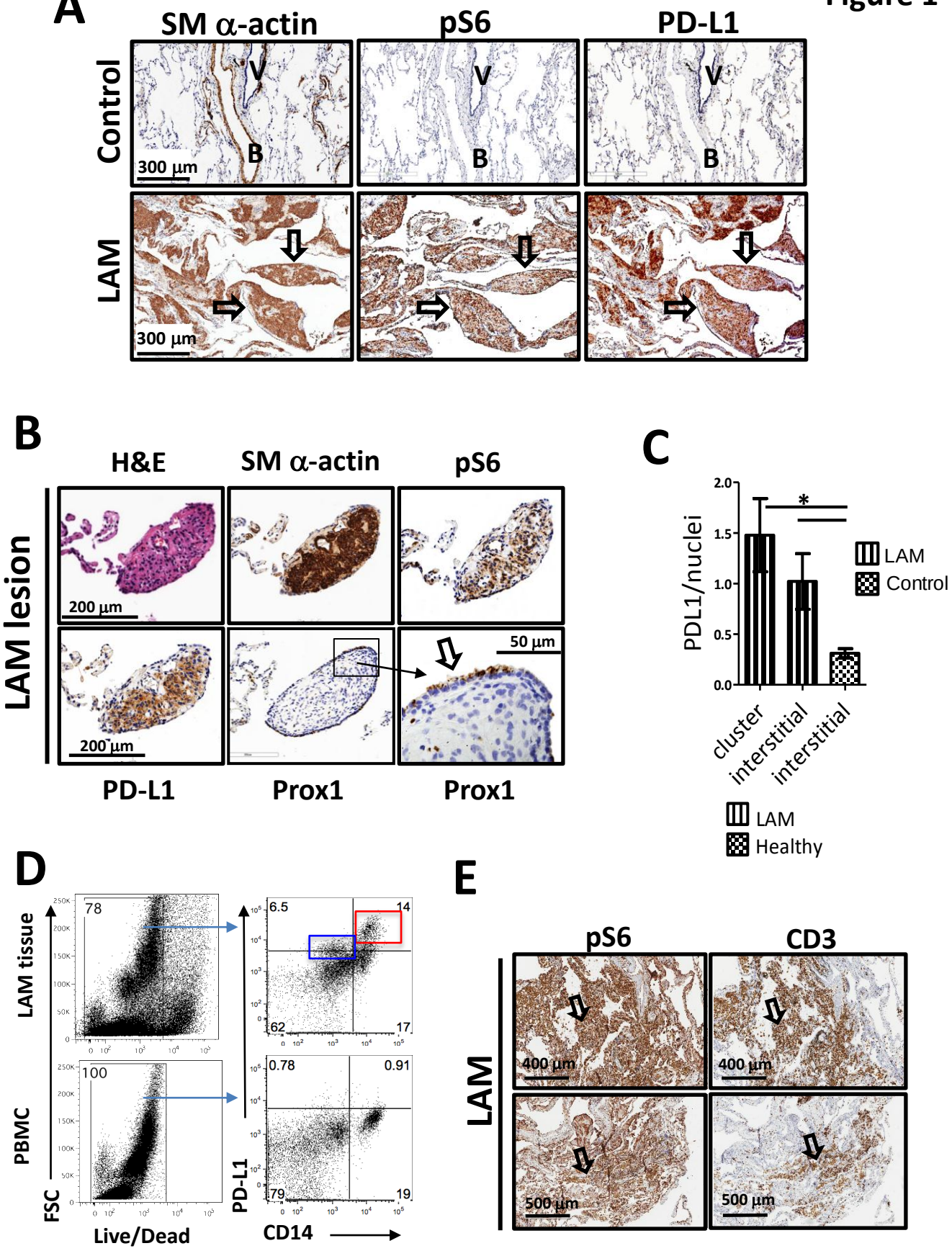


Copyright © 2018 by the American Thoracic Society

# Figure 2

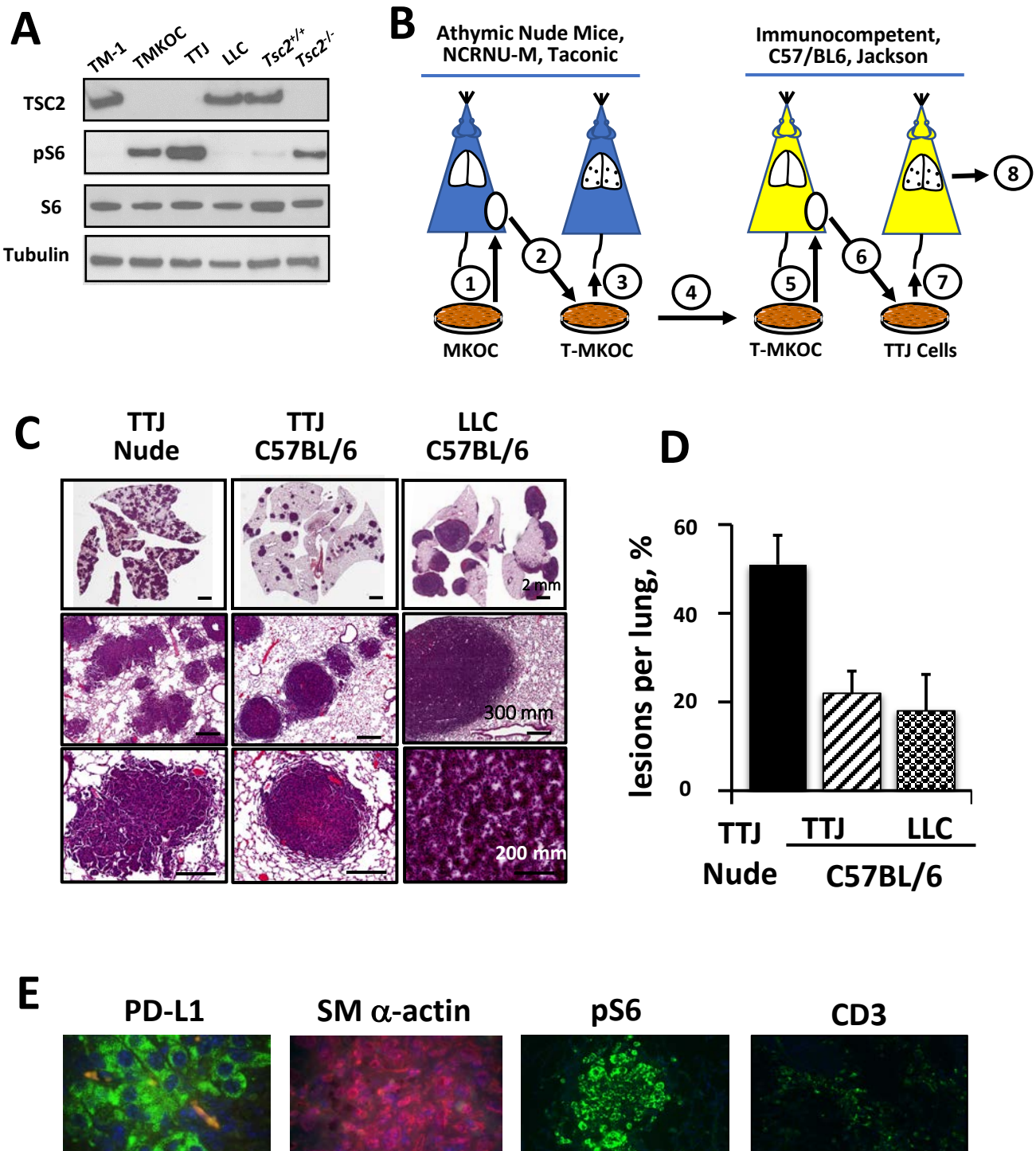


Copyright © 2018 by the American Thoracic Society

AJRCMB Articles in Press. Published on 10-August-2018 as 10.1165/rcmb.2018-0123OC

# Figure 3

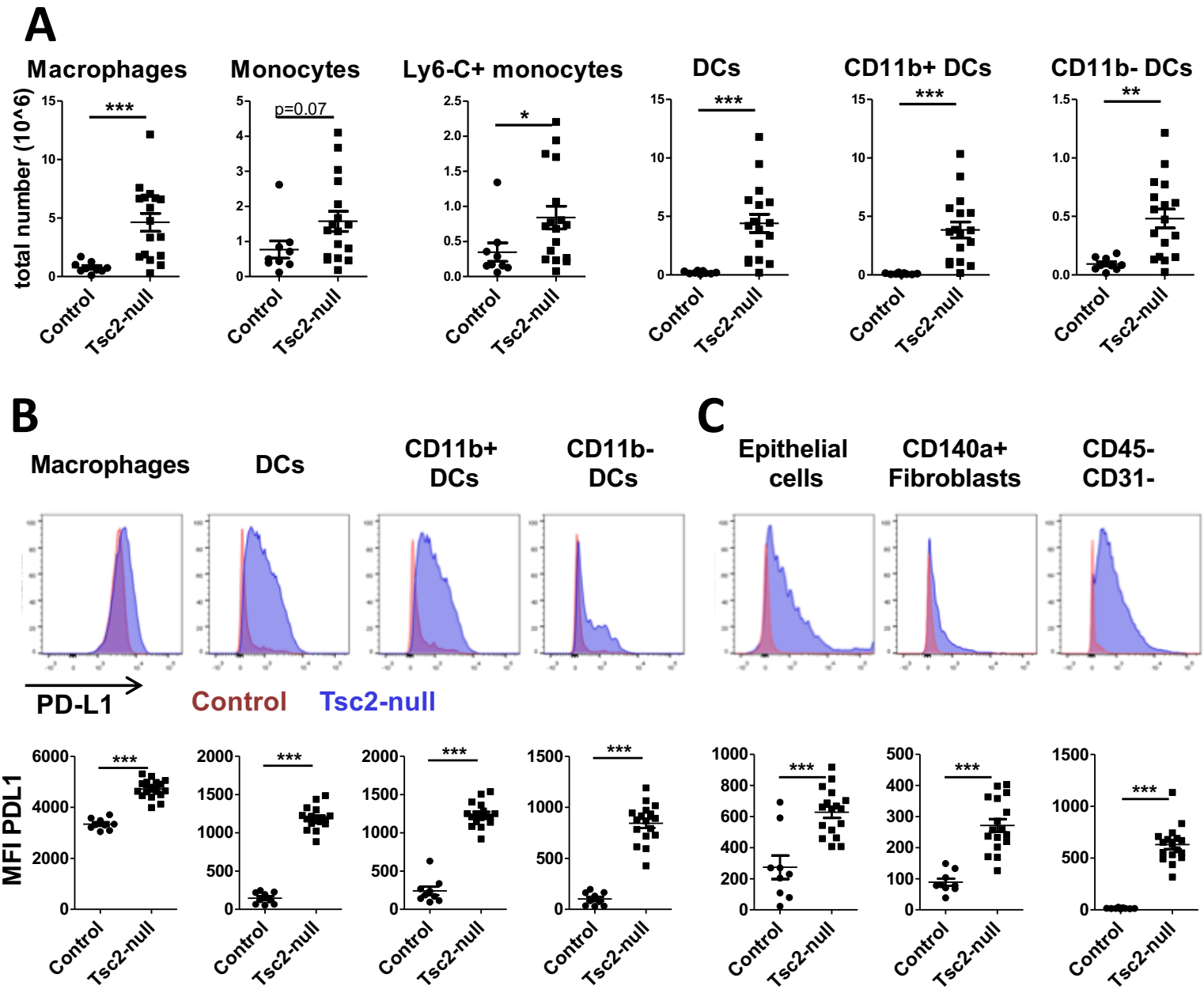


Copyright © 2018 by the American Thoracic Society

# Figure 4

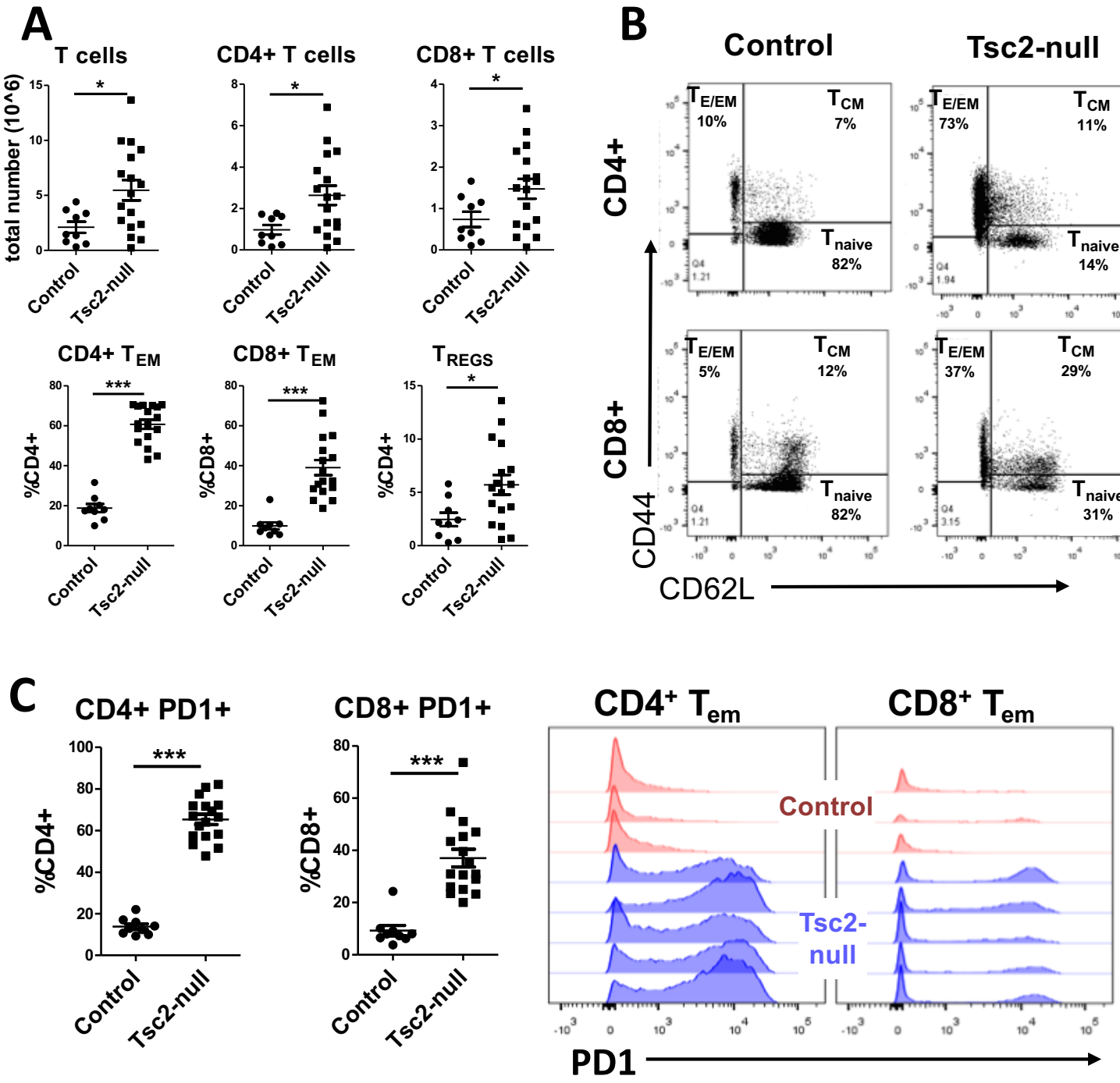


Copyright © 2018 by the American Thoracic Society

AJRCMB Articles in Press. Published on 10-August-2018 as 10.1165/rcmb.2018-0123OC

Figure 5

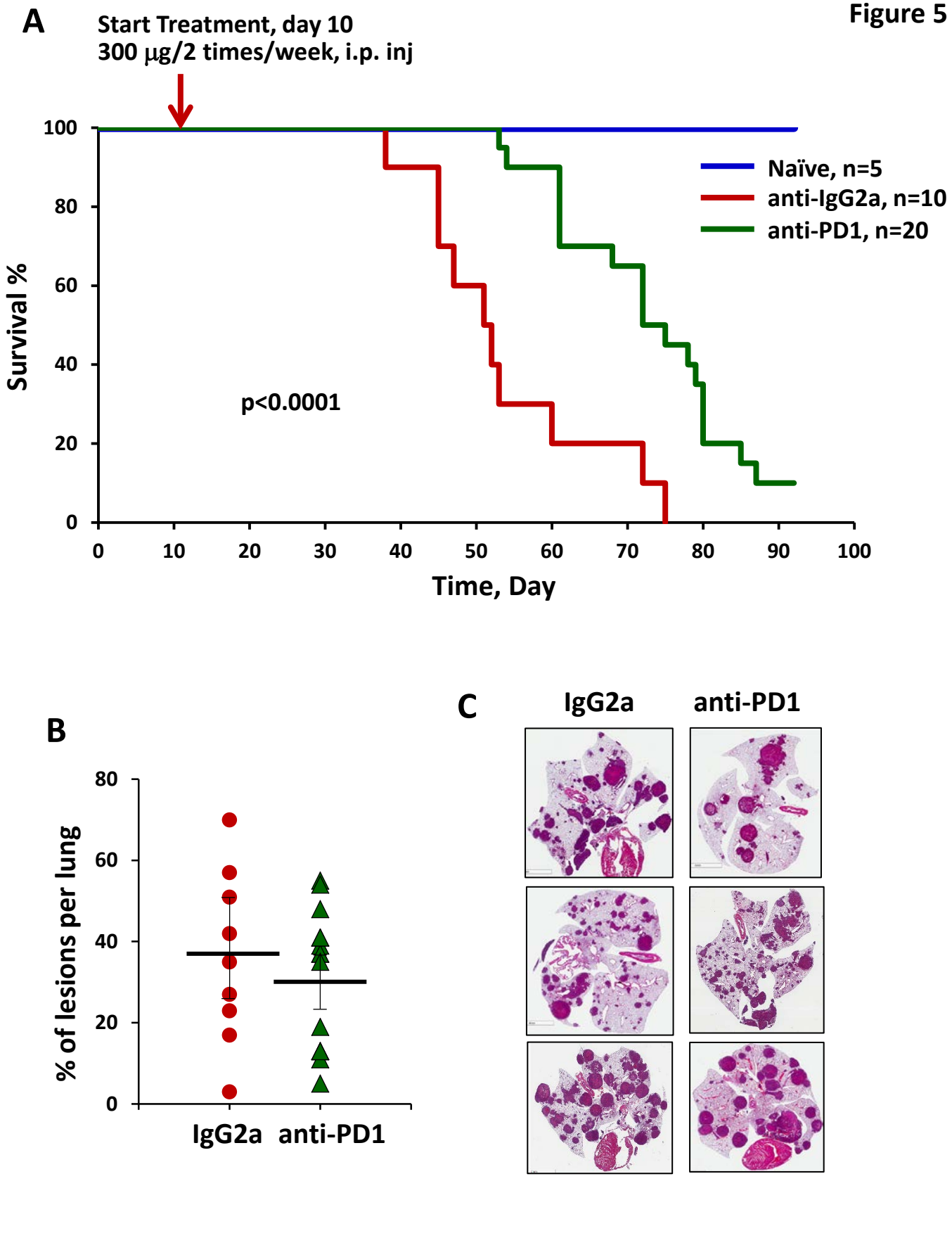


Copyright © 2018 by the American Thoracic Society

AJRCMB Articles in Press. Published on 10-August-2018 as 10.1165/rcmb.2018-0123OC



# Online Data Supplement

## Immune Checkpoint Ligand PD-L1 is Upregulated in Pulmonary Lymphangioleiomyomatosis (LAM)

Katharina Maisel, Mervyn J. Merrilees, Elena N. Atochina-Vasserman, Lurong Lian, Kseniya Obraztsova, Ryan Rue, Alexander N. Vasserman, Ning Zuo, Luis F. Angel, Andrew J. Gow, Inkyung Kang, Thomas N. Wight, Evgeniy Eruslanov, Melody A. Swartz, and Vera P. Krymskaya



Copyright © 2018 by the American Thoracic Society

AJRCMB Articles in Press. Published on 10-August-2018 as 10.1165/rcmb.2018-0123OC

## Supplemental Materials

### Materials and Methods

**Image Analysis.** Immunohistochemistry images were color deconvoluted using FIJI ImageJ deconvolution software to separate eosin staining from marker-specific horseradish peroxide (HRP)-based color staining. Images were then thresholded to exclude background staining, % area of marker or nuclei in the images was calculated, and the ratio of the two was quantified for comparison. Threshold remained the same between all groups and images to ensure unbiased comparison. Statistical analysis of PD-L1 IHC analysis of LAM lung (n=6) and control lung (n=4) was performed by student's *t*-test.

**Cell culture.** Tsc2-null cells derived from kidney lesions of $Tsc2^{+/-}$ mice were generously provided by Dr. Okio Hino (1). Mouse Tsc2-expressing Lewis Lung Carcinoma (LLC) and Tsc2-expressing mouse kidney tubular epithelial M1 cells were purchased from the ATCC. $Tsc2^{-/-}p53^{-/-}$ and $Tsc2^{+/+}p53^{-/-}$ mouse embryonic fibroblasts (MEFs) were generously provided by Dr. David J. Kwiatkowski. All cells were maintained in DMEM supplemented with penicillin/streptomycin, L-glutamine and 10% FBS.

**Animal Model.** To develop the experimental metastatic model of LAM in immunocompetent C57BL/6 mice, we used Tsc2-null TTJ cells (Figure 2A). TTJ cells were generated by successive propagation of the original Tsc2-null MKOC cells derived from mouse kidney lesions that spontaneously develop in heterozygous $Tsc2^{+/-}$ mice (1, 2) as schematically represented in Figure 2B. Briefly, $5x10^6$ cells were injected subcutaneously into flanks of NCRNU-M female athymic BALB/c-derived nude mice



Copyright © 2018 by the American Thoracic Society

(Figure 2B, Step 1). After tumors reached ~1.5 cm in diameter, mice were sacrificed and the tumors cells dissociated (Step 2). After 2 days in culture, the Tsc2-null cells from the primary tumors were resuspended in PBS, and $1x10^6$ cells were injected into tail vein (Step 3) of 8-week-old NCRNU-M athymic nude mice, which develop multiple Tsc2-null lung lesions as we demonstrated and described in our published study (3). To further edit immunogenicity of T-MKOC cells and enable their growth in immunocompetent mice, we then injected $5x10^6$ T-MKOC cells subcutaneously into both flanks of C57BL/6 mice (Jackson Labs, Bar Harbor, ME, USA) (Figure 2B, yellow, Step 5). When tumors reached ~1.5 cm in diameter, mice were sacrificed, the tumors were removed, enzymatically digested and plated in cell culture dishes in DMEM supplemented with 10% FBS (Figure 2B, yellow, Step 6). After 2 days in culture, the Tsc2-null cells from the primary tumors were resuspended in PBS, filtered, and $1x10^6$ cells were injected into the tail vein (t.v.) of 8-week-old C57BL/6 mice (Figure 2B, yellow, Step 7). These cells were named TTJ (Figure 2B, Step 7). Animals were observed twice a week by monitoring their weights. As seen in Figure E1, nude mice with TTJ and LLC cells were progressively losing weight from day 7 post-injection, and by day 17, they lost 15-20% of total weight. C57BL/6 mice with TTJ and LLC cells maintained their original weight while nude and C57BL/6 mice with TM1 cells gained weight. All animal groups were sacrificed at day 17 to compare tumor growth in nude and C57BL/6 mice (Figure E1).

As controls, we used Tsc2-expressing mouse kidney tubular epithelial TM1 cells and Lewis Lung Carcinoma (LLC) cells, an established model of mouse lung cancer. TM1 cells were generated by subcutaneous injection of M1 cells purchaced from ATCC. Briefly, $1x10^6$ M1 cells were injected into each flank of C57BL/6 mice. When tumors



Copyright © 2018 by the American Thoracic Society

AJRCMB Articles in Press. Published on 10-August-2018 as 10.1165/rcmb.2018-0123OC

reached ~1.5 cm in diameter, mice were sacrificed, tumors were resected, then enzymatically digested and maintained in cell culture in complete DMEM.

**Flow Cytometry.** For *in vitro* experiments, cells were cultured for 12-24hh with or without IFNγ, or 250 nM torin or diluent, and subsequently harvested and stained for PD-L1 and/or MHCI proteins. For *in vivo* experiments, mice were sacrificed after 3-4 weeks and lungs were digested for flow cytometric analysis. First, lungs were minced into 1-2-mm pieces, then suspended in DMEM containing 5% FBS and 1.2 mM $CaCl_2$ with 1 mg/mL collagenase D (Roche, Basel, Switzerland) and 300 U/mL collagenase IV (Worthington Biochemical, Lakewood, NJ, USA) for 1h at 37°C. To identify listed cell types, lysates were stained for CD3, CD4, CD8, CD44, CD62L, Foxp3, PD-L1, F4-80, CD11b, CD11c, Ly6C, Ly6G, CD45, CD31, gp38, EpCAM, MHCII, and CD140a. T cells were identified as CD3+ and either CD4+ or CD8+, with effector memory, central memory, and naïve T cells being Foxp3- and CD44+CD62L-, CD44+CD62L+, or CD44-CD62L+, respectively. Regulatory T cells were classified as CD3+CD4+Foxp3+. Stromal cells were identified as CD45- and CD31+ (endothelial cells), EpCAM+ (epithelial cells), CD140a+ (fibroblasts), or EpCAM-CD140a-CD31- (in the mouse model of LAM, this fraction contains mostly Tsc2-null cells). Antigen-presenting cells were identified as: neutrophils (CD11b+, Ly6G+), dendritic cells (CD11c+, $MHCII^{hi}$, and either CD11b+ or CD11b-), macrophages (CD11c+, $MHCII^{mid}$), monocytes ($CD11c^{lo-mid}$, CD11bhi, $SSC^{lo}$, and Ly6C+ or Ly6C-).

For human lungs, cells were stained for PD-L1 as well as CD14 to identify monocytic-derived cells as well as overall PD-L1 expression in cells. To exclude dead



Copyright © 2018 by the American Thoracic Society

cells from analysis, cells were stained with LIVE/DEAD® fixable dead cell stains (Molecular Probes, Life Technologies, Waltham, MA, USA).

**Western blotting.** Protein lysates from TM-1, TMKOC, TTJ, LLC cells, *Tsc2*$^{-/-}$ and *Tsc2*$^{+/+}$ MEFs were prepared using RIPA lysis buffer, resolved on 4-12% Bis-Tris SDS polyacrylamide gels (Life Technologies, Carlsbad, CA, USA), transferred to nitrocellulose followed by immunoblotting with either ribosomal protein S6, phospho-S6 (pS6), TSC2 or tubulin antibodies (Cell Signaling Technology, Danvers, MA, USA).

**qRT-PCR.** TM-1, TMKOC, TTJ, LLC cells, *Tsc2*$^{-/-}$ and *Tsc2*$^{+/+}$ MEFs were grown to near confluence, serum-deprived for 2h in 0.1% BSA, then either pretreated with 250 nM torin or diluent for 2h, followed by treatment with 100 U/ml mouse IFNγ for 24h, and qPCR analysis using the ΔΔCt method (4).



Copyright © 2018 by the American Thoracic Society

AJRCMB Articles in Press. Published on 10-August-2018 as 10.1165/rcmb.2018-0123OC

## References

1. Kobayashi T, Minowa O, Kuno J, Mitani H, Hino O, Noda T. Renal carcinogenesis, hepatic hemangiomatosis, and embryonic lethality caused by a germ-line tsc2 mutation in mice. *Cancer Res* 1999;59:1206-1211.
2. Kwiatkowski DJ. Animal models of LAM and tsc. *Lymph Res Biol* 2010;8:51-57.
3. Goncharova EA, Goncharov DA, Fehrenbach M, Khavin I, Ducka B, Hino O, Colby TV, Merrilees MJ, Haczku A, Albelda SM, et al. Prevention of alveolar destruction and airspace enlargement in a mouse model of pulmonary lymphangioleiomyomatosis (LAM). *Science translational medicine* 2012;4(154):154ra134.
4. Goncharova EA, Goncharov DA, James ML, Atochina-Vasserman EN, Stepanova V, Hong SB, Li H, Gonzales L, Baba M, Linehan WM, et al. Folliculin controls lung alveolar enlargement and epithelial cell survival through e-cadherin, lkb1, and ampk. *Cell reports* 2014;7(2):412-423.



Copyright © 2018 by the American Thoracic Society

**Figure E1**

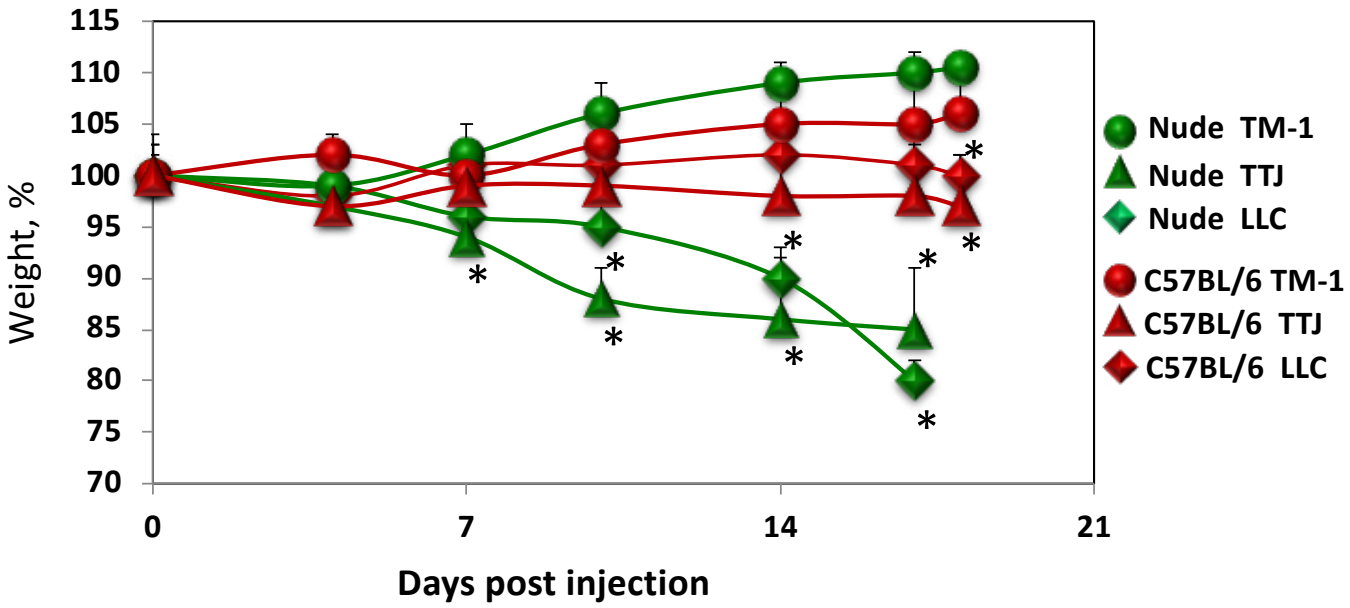


**Figure E1:** Nude (green) and C57BL/6J (red) mice were injected with $10^6$ TM1, TTJ or LLC cells. Mouse weights were monitored twice a week. Data are means ± SE (n=5 for each group).

Copyright © 2018 by the American Thoracic Society

AJRCMB Articles in Press. Published on 10-August-2018 as 10.1165/rcmb.2018-0123OC

**Figure E2**

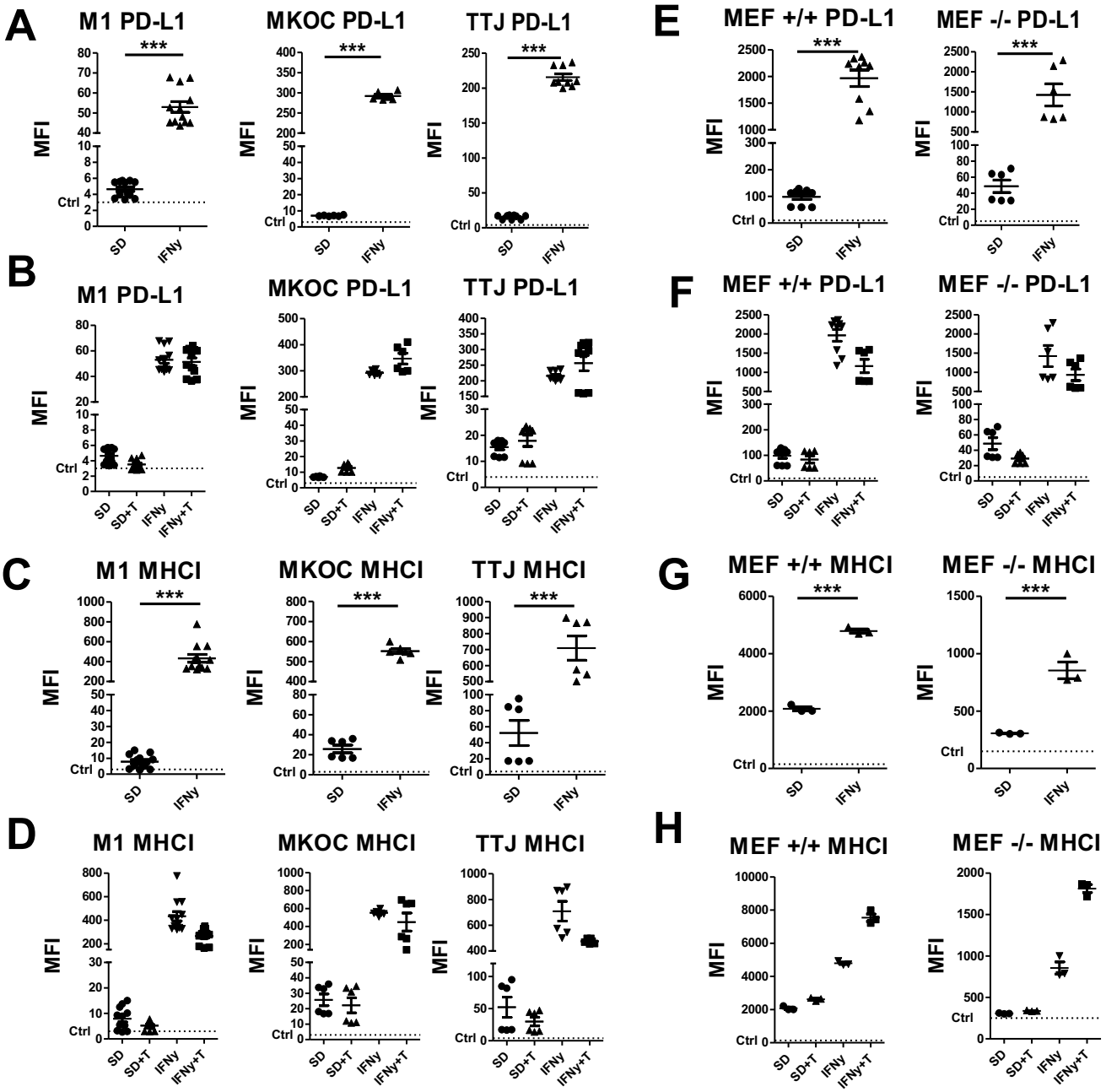


**Figure E2: Inhibition of mTORC1 has little effect on IFNγ-induced upregulation of PD-L1.** M-1, MKOC and TTJ upregulate PD-L1 and MHCI after stimulation with IFNγ (A,C), which is minimally affected by mTOR inhibition with 250 nM Torin (B,D). *Tsc2*$^{-}$/- (MEF -/-) and *Tsc2*$^{+/+}$ MEFs (MEFs +/+) upregulate PD-L1 and MHCI after stimulation with IFNγ (E,G) and there is a small decrease in PD-L1 but increase in MHCI expression upon mTOR inhibition (F, H). SD indicates samples treated with vehicle controls and T indicates treatment with mTOR inhibitor torin. Statistical analysis was performed as student's t-test with significance at $p < 0.05$ (n=3 samples, n≥2 experiments).

Copyright © 2018 by the American Thoracic Society

**Figure E3**

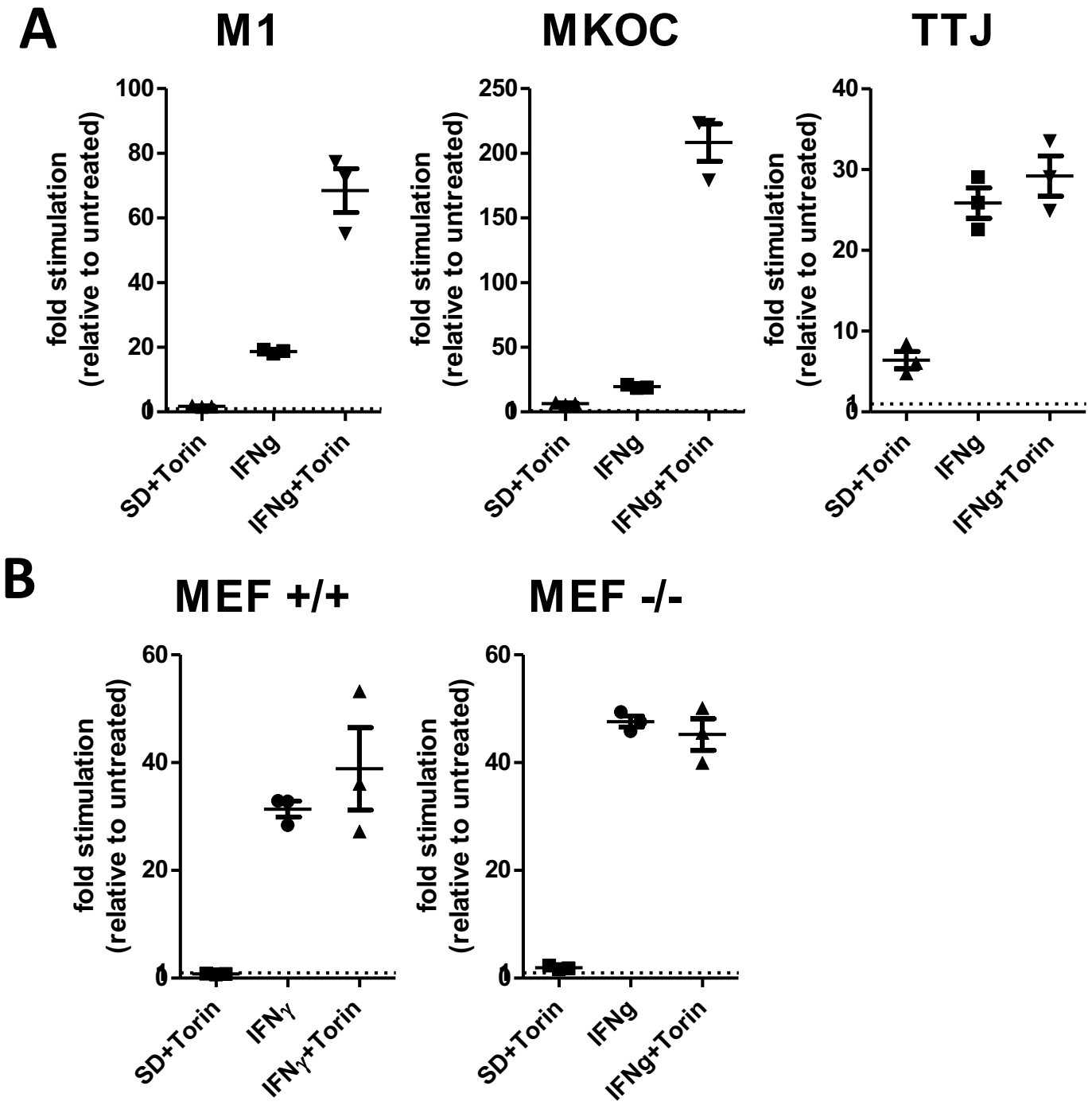


**Figure E3: Inhibition of mTORC1 with torin has little effect on IFNγ-induced upregulation of PD-L1 mRNA in Tsc2-null cells**. M1, MKOC, TTJ, LLC cells, *Tsc2*$^{-/-}$ and *Tsc2*$^{+/+}$ MEFs were growth to near confluence, serum-deprived for 2 hr in 0.1% BSA, then either pretreated with 250 nM Torin or diluent for 2 hr, followed by treatment with 100U/ml mouse IFNγ for 24 hr, and qPCR analysis. Data are representative of n=3 samples per group and 2 separate experiments.

Copyright © 2018 by the American Thoracic Society

AJRCMB Articles in Press. Published on 10-August-2018 as 10.1165/rcmb.2018-0123OC

**Figure E4**

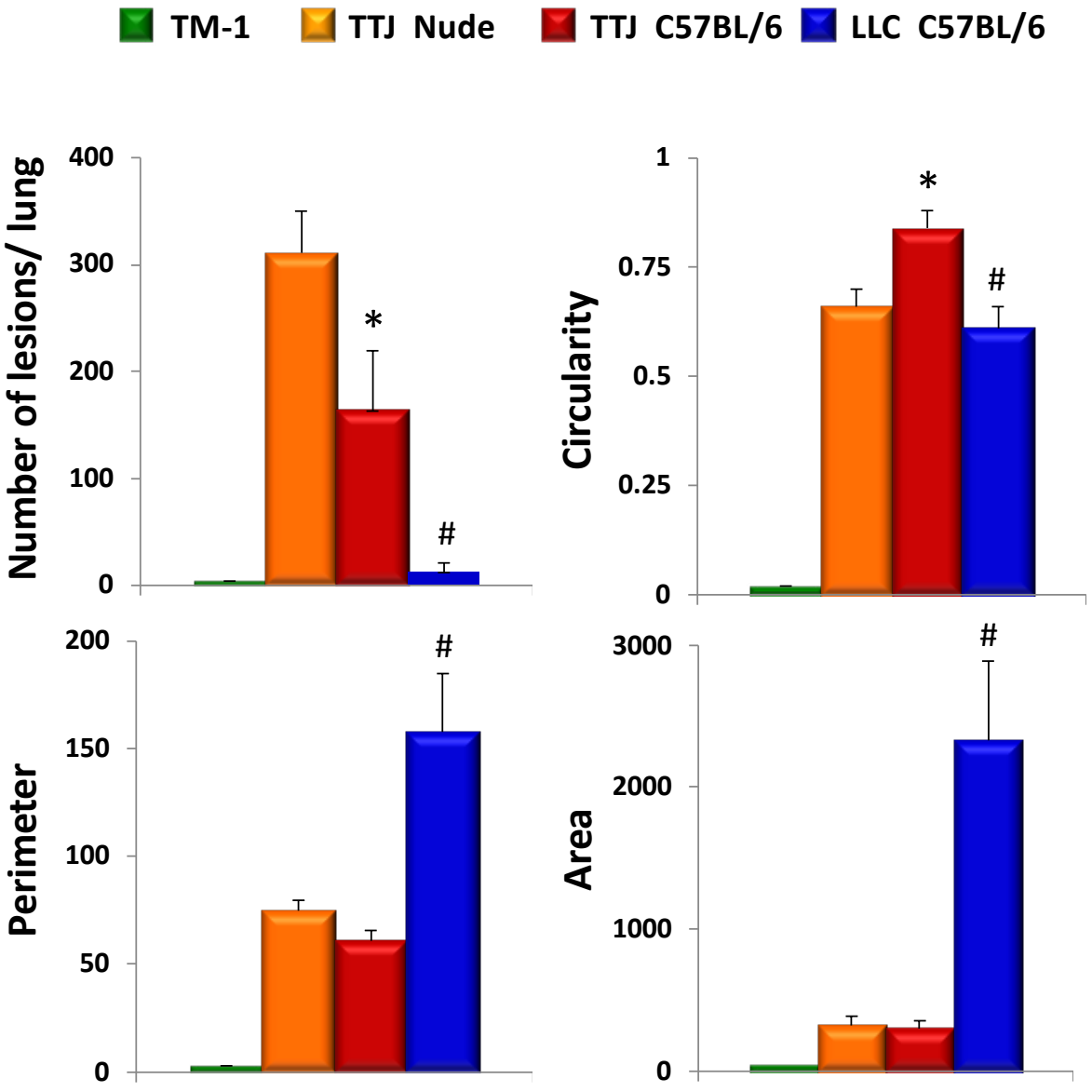


**Figure E4: Tsc2-null TTJ lesion number and shape differ in nude and C57BL/6 mice.** H&E-stained sections of the whole lung were scanned to create digital whole slide images (WSI) using an Aperio ScanScope XT (Aperio Technologies, Vista, CA) with ×20 magnification (0.46 um per pixel). Each WSI was evaluated using Aperio ImageScope software, ImageJ and Photoshop to quantify the number, circularity, perimeter and area of lesions.

Copyright © 2018 by the American Thoracic Society

# Figure E5

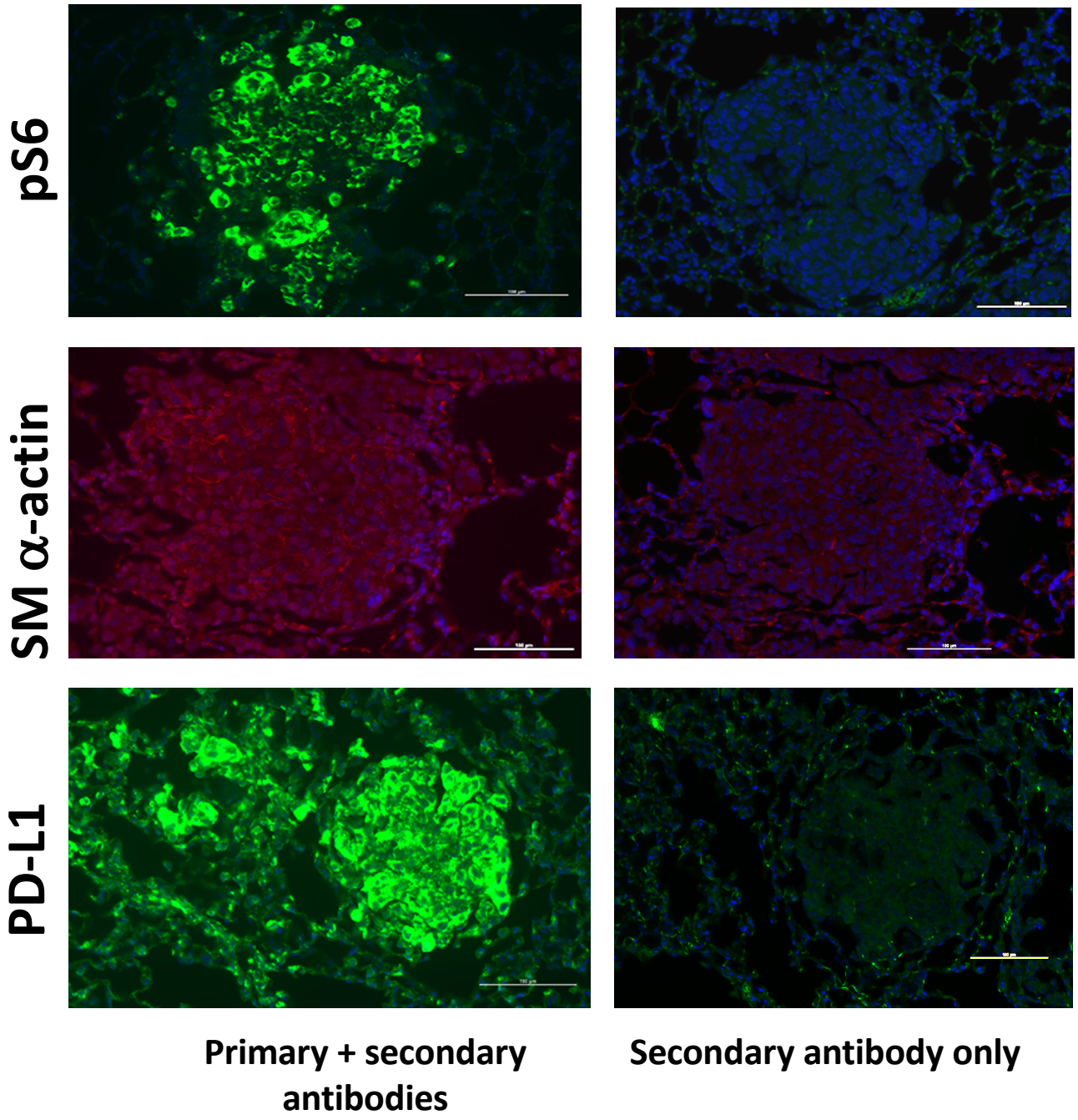


**Figure E5:** IHC analysis of pS6, SM α-actin, and PD-L1 expression in C57BL/6 mouse lungs with Tsc2-null lung lesions (n=3). Left panels represent images stained with specific primary and secondary antibodies. Right panels represents consecutive slides stained with secondary antibodies only. Scale bars – 100 μM.

Copyright © 2018 by the American Thoracic Society